Nucleated wetting films: The late-time behavior

Bruce M. Law
Department of Physics, Kansas State University, Manhattan, Kansas 66506-2601
(Received 11 February 1993)

We examine the late-time wetting behavior of the system hexadecane plus acetone after the coalescence of nucleated wetting droplets into a uniform wetting film. The experimental results at large reduced temperatures ($t > 7\times10^{-4}$) fall into two distinct wetting layer thicknesses of 43.1±2.7 nm and 29.5±2.0 nm. We identify the ~43.1 nm layer with a nonequilibrium wetting state that exists after the nucleated wetting droplets have coalesced into a uniform wetting film. This nonequilibrium state has a lifetime of a few hours before it collapses into a film of thickness ~29.5 nm, which we believe corresponds to an equilibrium wetting layer. The collapse of the nonequilibrium wetting film is explained in terms of a hydrodynamic instability where the film is in a regime that is unstable to long-wavelength capillary wave fluctuations on the adjacent critical interface. The magnitude of the equilibrium wetting film gives reasonable quantitative agreement with the dispersion theory of Dzyaloskinskii, Lifshitz, and Pitaevskii [Adv. Phys. **10**, 165 (1961)]. At small reduced temperatures ($t < 7\times10^{-4}$) critical adsorption effects within the wetting layer become significant.

PACS number(s): 68.10.−m, 68.15.+e, 66.10.Ed

I. INTRODUCTION

Since the seminal papers of Cahn [1] and Ebner and Saam [2] in 1977, which predicted the occurrence of a wetting transition at the critical fluid-vapor (or critical fluid-solid) surface in the two phase region, an intense experimental and theoretical effort [3] has been expended in understanding the equilibrium properties of the wetting layer. In Fig. 1(a) we show the heavier β phase wetting the upper liquid-vapor (αv) surface of a critical binary liquid mixture where the equilibrium wetting layer thickness d is determined by gravity (which thins the layer) and dispersion forces (which thicken the layer). Despite this effort there are many reports in the literature [4] which state that the measured wetting layer properties disagree with some of the predictions of the Dzyaloskinskii-Lifshitz-Pitaevskii (DLP) theory of dispersion forces [5]. Unfortunately these claims have often been based upon simplified estimates from this theory rather than the complete theory.

Complications arise when trying to compare experimental data with theory very close to the critical temperature (T_c): (i) One must correctly model the divergence of the critical $\alpha\beta$ interface adjacent to the wetting layer, and (ii) critical adsorption effects are expected to become important near T_c. Surprisingly, it is not even known experimentally whether in fact a wetting layer continues to exist for sufficiently small reduced temperatures ($t = |T - T_c|/T_c$) when the correlation length (ξ) is much greater than the wetting layer thickness.

In a previous publication [6] we observed the new phenomenon of nucleated wetting at a critical binary liquid-vapor surface; where upon quenching the critical liquid mixture hexadecane plus acetone from the one phase region into the two phase region wetting droplets of the heavier acetone-rich phase were observed to nucleate at the upper liquid-vapor surface [Fig. 1(b)]. The purpose of this publication is to interpret the results from this experiment *at late times* after the wetting droplets have coalesced into a uniform wetting film. We compare the measured values of the wetting layer thickness with the predictions of the DLP theory and also examine when critical adsorption effects become important. An issue that has not previously been addressed in the literature, with regard to wetting layers, but which is especially important for mixtures where one component is polar and consequently has a large static dielectric constant is the influence of impurity ions on the dispersion force [7]. A large static dielectric constant gives rise to a large zero-frequency component to the dispersion force; however the presence of mobile impurity ions in solution can screen out this zero-frequency component if the Debye screening length is smaller than the wetting layer thick-

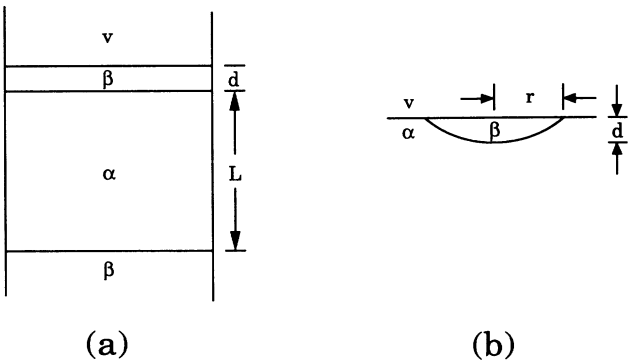

FIG. 1. (a) Schematic diagram of the heavier β phase wetting the upper liquid-vapor (αv) surface. The wetting layer has a thickness d while the bulk α phase has a height of L. (b) Schematic diagram of a nucleated wetting droplet of the heavier β phase at the αv surface. The droplet has a lateral radius r and thickness d.

ness [8].

In Sec. II we examine the DLP theory of dispersion forces for the critical liquid mixture hexadecane plus acetone and also consider how mobile impurity ions alter this dispersion force. We examine the experimental data (Sec. III) and show that the data cannot be understood in terms of a uniform film with composition β very close to T_c ($t \leq 7\times10^{-4}$); namely, critical adsorption effects become important. The data for $t > 7\times10^{-4}$ are analyzed in terms of a Fisk-Widom wetting layer model; the data are observed to fall into two wetting layer thickness of $\sim$43.1 nm and $\sim$29.5 nm. The thicker film corresponds to a layer just after droplet coalescence to a thick film; this film ruptures to the thinner film after $\sim 2.3\times10^4$ s. The thinner film is believed to correspond to an equilibrium wetting layer and is therefore compared with the theoretical calculations of Sec. II. An explanation for the thick film instability is suggested in Sec. IV. We conclude this paper, in Sec. V, with a discussion of our results.

II. DISPERSION FORCE

The equilibrium wetting layer thickness d, at the binary liquid-vapor surfaces in the two phase region, is determined by the solution to the equation [9,10]

$$F(d)+\Delta\rho g L = 0 , \tag{1}$$

where $F(d)$ is the dispersion force; $\Delta\rho=\rho_\beta-\rho_\alpha$ is the mass density difference between the β and α phases, g is the acceleration due to gravity, and L is the height of the bulk α phase. For an equilibrium wetting layer to exist, the dispersion force $F(d)$ must be negative [9,10] where according to the DLP theory for arbitrary media 1, 2, and 3 corresponding to v, α, and β above

$$F(d)=(k_B T/\pi c^3)\sum_{j=0}^{\infty}{}' \varepsilon_3^{3/2}\xi_j^3\int_1^\infty p^2 dp\{[f_1(1)f_2(1)\exp(2p\xi_j\varepsilon_3^{1/2}d/c)-1]^{-1} + [f_1(\varepsilon_1/\varepsilon_3)f_2(\varepsilon_2/\varepsilon_3)\exp(2p\xi_j\varepsilon_3^{1/2}d/c)-1]^{-1}\} , \tag{2a}$$

where

$$f_i(x)=(s_i+px)/(s_i-px) \tag{2b}$$

and

$$s_i=(\varepsilon_i/\varepsilon_3-1+p^2)^{1/2}, \quad i=1,2 . \tag{2c}$$

The quantity k_B is Boltzmann's constant, c is the speed of light, $\xi_j=2\pi j k_B T/\hbar$, $2\pi\hbar$ is Planck's constant, and ε_1, ε_2, and ε_3 are the frequency-dependent dielectric constants $\varepsilon=\varepsilon(i\xi_j)$ of the three media evaluated at the imaginary frequencies $\omega=i\xi_j$. The prime attached to the summation denotes that the term with $j=0$ is to be given half weight.

The dielectric constant for phases 2 and 3, $\varepsilon_2(i\xi_j)$ and $\varepsilon_3(i\xi_j)$, are calculated from the Clausius-Mossotti relation

$$f(\varepsilon_i(i\xi))=\Omega_i[\phi_i f(\varepsilon_A(i\xi))+(1-\phi_i)f(\varepsilon_B(i\xi))] , \quad i=2,3 , \tag{3a}$$

where

$$f(x)=(x-1)/(x+2) , \tag{3b}$$

Ω_i originates from the volume change on mixing and ϕ_i is the volume fraction of A molecules (in a mixture of A and B molecules). Here $\varepsilon_A(i\xi_j)$ and $\varepsilon_B(i\xi_j)$ are the dielectric constants for the pure liquids determined from the equation

$$\varepsilon(i\xi)=1+(\varepsilon_{vis}-1)/[1+(\xi/\omega_{uv})^2] + (\varepsilon_{0+}-\varepsilon_{vis})/[1+(\xi/\omega_{ir})^2] \tag{4}$$

for all terms $j>0$ in (2). For the zero-frequency term of (2) ε_{0+} is replaced by $\varepsilon(0)$ in (4). The relevant parameters used in this calculation for the critical binary liquid mixture hexadecane plus acetone are listed in Tables I and II. We have followed very closely, in both notation and treatment, the excellent pedagogical paper of Kayser [10] for calculating $F(d)$ in a critical binary liquid mixture.

What is the effect of impurity ions in solution on the dispersion force $F(d)$ [7]? According to Mahanty and Ninham [8], *for uncharged surfaces,* mobile impurity ions will primarily affect the $j=0$ term in (2). This is because the frequency ξ_j for $j=1$ at room temperature is of order 10^{14} rad/sec and the massive impurity ions cannot follow this high frequency field. In the presence of impurity ions the $j=0$ force per unit area is given by [8]

$$F_{j=0}(d)=\frac{k_B T}{16\pi d^3}\int_0^\infty \frac{x s_3 dx}{[\Delta_{13}\Delta_{23}e^{-s_3}]^{-1}-1} , \tag{5a}$$

where

TABLE I. Pure liquid dielectric data.

Liquid	$\varepsilon(0)$	ε_{0+}	ε_{vis}	$10^{14}\omega_{ir}$ (rad/s)	$10^{16}\omega_{uv}$ (rad/s)
Acetone	21.2[a]	2.2[a]	1.819[b]	5.54[c]	1.8[b]
Hexadecane	2.04[d]	2.04[d]	2.025[e]	5.54[e]	1.85[c]

[a]Reference [22].
[b]Determined from a Cauchy plot [10] for acetone using data from [23].
[c]IR absorption band for C—H vibrations.
[d]We have assumed that $\varepsilon(0)=\varepsilon_{0+}$, as hexadecane is nonpolar, where $\varepsilon(0)$ is estimated from [22] by examining the variation of $\varepsilon(0)$ for the homologous series C_nH_{2n+2}.
[e]Reference [24].

TABLE II. Hexadecane plus acetone mixture data.

	Reference
Critical temperature, $T_c = 304.267$ K	
Critical volume fraction of hexadecane, $\phi_c = 0.4826$	[25]
Rectilinear diameter, $(\phi_2+\phi_3)/2 = \phi_c - 0.189t$	[25]
Coexistence curve, $\phi_2-\phi_3 = (-t)^{\beta}(2.26-1.5(-t)^{\Delta})$; $\beta=0.34$; $\Delta=0.5$	[25]
Volume change on mixing, $\Omega_i = 115.14/(115.14+V_i^E)$; $i=2,3$	[25]
$V_i^E = \phi_i(1-\phi_i)\sum_{n=0}^{5} a_n(1-2\phi_i)^n$	
$a_0=3.8105$; $a_1=-3.148$; $a_2=4.2388$; $a_3=0.0904$; $a_4=-5.8471$; $a_5=3.1686$	
Density difference, $\Delta\rho = 0.0375(-t)^{\beta}$ g/cm^3	a
Correlation length for $T>T_c$, $\xi_+ = 0.2t^{-\nu}$ nm, $\nu=0.63$	b
Correlation length amplitude ratio, $\xi_{+0}/\xi_{-0}=1.96$	[27]
Critical surface tension, $\sigma_{\alpha\beta}=50t^{\mu}$ erg/cm^2, $\mu=1.24$	c
Viscosity, $\eta \sim 1.8$ cp	[26]
Height of hexadecane-rich phase (α), $L \approx 0.56$ cm	

[a]Calculated from $\rho_i = \phi_i\rho_A + (1-\phi_i)\rho_B$ using the density data from [26].
[b]Determined in Reference [16].
[c]Determined using the experimental value for the amplitude ratio $R^{+}_{\sigma\xi} = \sigma_0(\xi_{+0})^2/k_BT_c$ [28].

$$\Delta_{ij} = \frac{\varepsilon_i(0)s_i - \varepsilon_j(0)s_j}{\varepsilon_i(0)s_i + \varepsilon_j(0)s_j}\ , \tag{5b}$$

$$s_j = \{x^2 + [2d\kappa_D(j)]^2\}^{1/2}\ , \tag{5c}$$

and the reciprocal Debye length κ_D is

$$\kappa_D^2(j) = \frac{e^2}{\varepsilon_j(0)\varepsilon_0 k_B T}\sum_i z_i^2\rho_i\ . \tag{6}$$

Here e is the electronic charge, z_i the valence of species i, ρ_i the number density of species i, and ε_0 the vacuum permittivity.

Ripple and Franck [11] measured an ion concentration of $\rho \sim 10^{23}$ m^{-3} in the critical binary liquid mixture nitromethane plus carbon disulfide where they assumed monovalent impurity ions of identical equivalent conductance in the two phases. The value of ρ corresponds to a Debye screening length of $\kappa_D^{-1} \sim 10$ nm. One can show from (5) that if $2\kappa_D d \gg 1$ then the impurity ions screen out the zero-frequency contribution to the dispersion force. For the wetting layers observed in the next section ($\sim$30–45 nm) the zero-frequency term would be screened out for the ion concentration measured by Ripple and Franck.

In Fig. 2 we plot $F(d)$ as a function of d for various reduced temperatures both with (solid symbols) and without (open symbols) the zero-frequency term ($j=0$). Henceforth we will label the dispersion force $F(d)$ if it includes the zero-frequency term and $F_>(d)$ if it does not. It is immediately obvious that the zero-frequency term is very large and positive. $F(d)$ changes sign at $d \sim 30$ nm for $10^{-4} \le t \le 10^{-2}$ and consequently thick wetting layers would be unstable [$F(d)>0$]. $F_>(d)$ is always negative therefore if the zero-frequency term is screened out the wetting layers would always be stable.

Equation (2) is rather cumbersome for obtaining an estimate of the sign and magnitude of the contributions to $F(d)$. Israelachvili [12] has given a simplified expression for (2), for nonretarded van der Waals forces ($d < 5$ nm), from which it is somewhat easier to understand the sign and magnitude of the contribution for the terms which enter $F(d)$. The essential conclusion is that the sign and magnitude of each contribution to the dispersion force is proportional to $(\varepsilon_1-\varepsilon_3)(\varepsilon_2-\varepsilon_3)$ at each frequency. Therefore from Table I we expect the $j=0$ contribution will be large and positive while the optical frequency contribution will be negative as expected. If the impurity ion concentration is sufficiently large it will play an important role in many of the wetting layer systems studied to date where one of the components has a large static dielectric constant.

III. EXPERIMENTAL RESULTS

In our previous study of nucleated wetting [6] we used ellipsometry to monitor the time development of

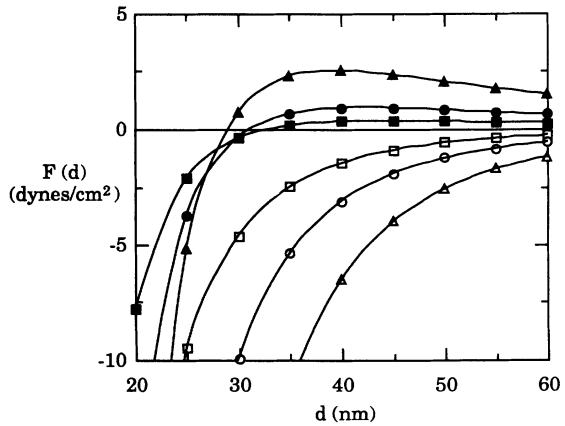

FIG. 2. Variation of the dispersion force per unit area $F(d)$ for critical hexadecane plus acetone as a function of the wetting layer thickness d at various reduced temperatures, $t = 10^{-2}$ (triangles), 10^{-3} (circles), and 10^{-4} (squares). The solid (open) symbols include (exclude) the $j=0$ contribution to $F(d)$.

$\bar{\rho}=\mathrm{Im}(r_p/r_s)$ at the Brewster angle after a temperature quench from the one phase region into the two phase region where r_p (r_s) is the reflection amplitude parallel (perpendicular) to the plane of incidence. It is well known that $\bar{\rho}$ is very sensitive to any surface structure and has a sensitivity of ~ 0.1 nm [13]. For the duration of an experiment the temperature was stable to ~ 5 mK after the initial temperature quench of time constant ~ 10 min.

In Fig. 3 we plot the late time $\bar{\rho}$ values at various reduced temperatures (open circles) after the nucleated wetting droplets have coalesced and settled into a uniform, reasonably time-independent wetting film. The typical error in $\bar{\rho}$ for the wetting layer is $\pm 1.5\times 10^{-4}$. On the same graph we have drawn in lines of constant wetting layer thickness calculated by solving Maxwell's equation for a Fisk-Widom model [14] of the wetting layer using a numerical matrix technique [15]. The Fisk-Widom model for the wetting layer has the following form for the optical dielectric constant:

$$\varepsilon(z)=\begin{cases}1, & z<0\\ \frac{1}{2}(\varepsilon_\alpha+\varepsilon_\beta)+\frac{1}{2}(\varepsilon_\alpha-\varepsilon_\beta)P\left[\dfrac{z-(d+2\xi_-)}{2\xi_-}\right], & z\geq 0\end{cases}, \quad (7a)$$

where

$$P(x)=\frac{\sqrt{2}\tanh(x)}{[3-\tanh^2(x)]^{1/2}}. \quad (7b)$$

Here we have assumed that the wetting layer has a composition identical to the bulk β phase and that the critical $\alpha\beta$ interface adjacent to the wetting layer develops fully over a distance of $4\xi_-$ before the layer is considered part of the wetting film. The correlation length in the two phase region ξ_-, was determined from the universality of the critical adsorption curve in the one phase region [16] and the correlation length amplitude ratio (Table II) while ε_α and ε_β were calculated from the Clausius-Mossotti relation (3) using the refractive index for this mixture at the He-Ne laser wavelength of 632.8 nm used in the ellipsometer.

From Fig. 3 we observe that for $t\leq 7\times 10^{-4}$ the experimental data cannot be explained in terms of the Fisk-Widom wetting model (7). Critical adsorption effects [17,18], which cause an enhancement in the concentration of acetone at the liquid-vapor surface, must be responsible for the large values of $\bar{\rho}$ observed at these small values of t. We have not attempted to incorporate critical adsorption effects within the wetting layer model as this would involve a complicated matching procedure in both $\varepsilon(z)$ and $d\varepsilon/dz$ between the adsorption profile and the Fisk-Widom wetting profile [18]. Our current analysis technique involves no free parameters and appears to be applicable for $t>7\times 10^{-4}$ thus allowing the experimental data to be compared directly with the DLP theory.

In Fig. 4 we compare the experimental wetting layer thicknesses (open symbols) deduced from Fig. 3 with the theoretical predictions of Sec. II in the absence of impurity ions (solid line). The solid line was calculated using the results in Table II to determine $-\Delta\rho gL$ and then the value of d was determined from the intersection of $-\Delta\rho gL$ and $F(d)$ in Fig. 2, for each reduced temperature, as prescribed by Eq. (1). The experimental data appears to fall into two groups clustered around the average thicknesses of 43.1 ± 2.7 nm and 29.5 ± 2.0 nm where the typical error associated with each individual data point was ± 1.5 nm for $d\sim 43.1$ nm and ± 1.0 nm for $d\sim 29.5$ nm. The origin of the two experimental wetting thicknesses observed in Fig. 4 can be understood from Fig. 5 where we show a wetting layer temperature quench

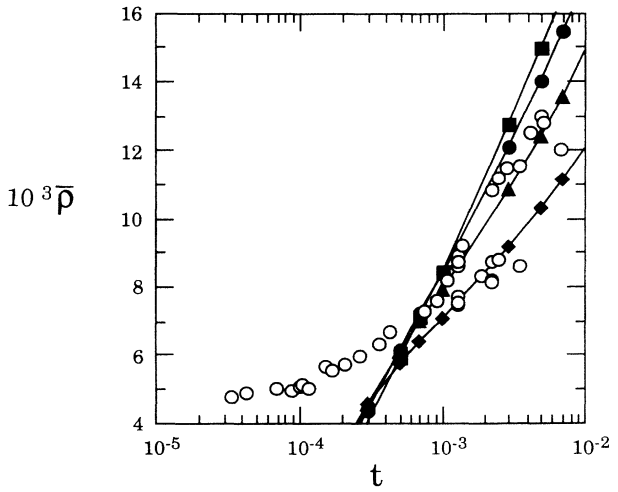

FIG. 3. The late-time ellipticity $\bar{\rho}$ (open circles) for critical hexadecane plus acetone at various reduced temperatures t. Also plotted on the same graph are lines of constant wetting layer thickness d determined from the Fisk-Widom wetting layer model [Eq. (7)]: $d=30$ nm (solid diamonds), 40 nm (solid triangles), 50 nm (solid circles), and 60 nm (solid squares).

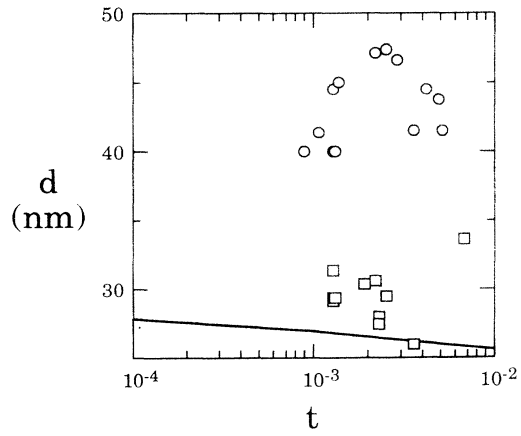

FIG. 4. Comparison of the experimental wetting layer thicknesses (open symbols) with the predictions from the DLP theory in the absence of impurity ions (solid line). The experimental data falls into two distinct groups with thicknesses of ~ 43.1 nm (open circles) and ~ 29.5 nm (open squares). The thicker wetting layer corresponds to a nonequilibrium wetting film which eventually collapses to the thinner equilibrium wetting film.

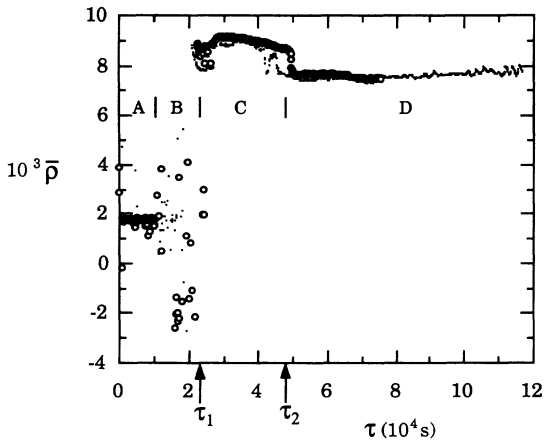

FIG. 5. Variation of $\bar{\rho}$ with time τ after a temperature quench from the one phase into the two phase region at $\tau=0$ s to a reduced temperature of $t=1.3\times10^{-3}$ for two independent experiments (dots and open circles). Metastable surface state (A), nucleation and growth of wetting droplets (B), nonequilibrium wetting layer of thickness $d\sim43.1$ nm (C), and equilibrium wetting layer of thickness $d\sim29.5$ nm (D). The wetting droplets coalesce to a nonequilibrium wetting layer at time τ_1. This nonequilibrium wetting layer undergoes a hydrodynamic instability to the equilibrium wetting layer at time τ_2 where the film rupture time $\tau_r=\tau_2-\tau_1\sim2.3\times10^4$ s.

experiment which includes both of these wetting layer thicknesses. The system was quenched from the one phase region into the two phase region at time $\tau=0$ s. Figure 5 exhibits all of the features discussed in our earlier publication [6], namely, a peak in $\bar{\rho}$ near $\tau=0$ s which we believe signifies spinodal wetting, a metastable surface state (region A), a nucleation and growth of wetting droplets phase (region B), and a uniform wetting film phase (region C). The uniform film phase has a thickness of ~43.1 nm, however, at $\tau\sim5\times10^4$ s this phase suddenly collapses to a wetting layer film of thickness ~29.5 nm (region D). This behavior is very reproducible as demonstrated by the dots and open circles in Fig. 5.

In our previous publication on nucleated wetting [6] we interpreted region C as the region where droplets had coalesed into a uniform nonequilibrium wetting film which over time would eventually decrease *smoothly* to the equilibrium film thickness. Many experimental runs were terminated in region C after a few hours without knowing of the existence of region D. We believe region D with a thickness of 29.5 ± 2.0 nm represents the equilibrium wetting layer because it remains reasonably constant over an extended period of time (~20 h). This wetting layer thickness agrees reasonably well with the DLP model in the absence of impurity ions (solid line in Fig. 4) where d varies from 25.4 nm at $t=10^{-2}$ to 26.8 nm at $t=10^{-3}$. We believe that the discrepancy observed between theory and experiment for the equilibrium wetting layer in Fig. 4 is either due to our neglect of critical adsorption effects or due to the uncertainty associated with the dielectric dispersion $\varepsilon(\omega)$ assumed for this critical liquid mixture. We do not believe that the difference between theory and experiment is due to the screening effects of impurity ions considered in Sec. II. We will examine this point further in Sec. V.

IV. HYDRODYNAMIC INSTABILITY

What is the physical mechanism for the sudden collapse of the nonequilibrium wetting layer, regions C to D in Fig. 5? Region C corresponds to a wetting layer thickness of ~43.1 nm. This thickness lies in the region where $F(d)$ is positive and $\partial F(d)/\partial d$ is negative (Fig. 2) and therefore the wetting layer is unstable to long wavelength capillary wave fluctuations on the adjacent critical $\alpha\beta$ interface [19,20]. Peristaltic capillary waves within the wetting layer have a dispersion relation given approximately by [20]

$$\omega^2\approx\frac{k^2d}{\rho_\beta}\left[k^2\sigma_{\alpha\beta}+\frac{\partial F(d)}{\partial d}\right], \tag{8}$$

where k is a two-dimensional surface wave number, ρ_β is the wetting layer density, and $\sigma_{\alpha\beta}$ is the critical interfacial tension. The nonequilibrium wetting layer thickness is in the regime where $\partial F/\partial d<0$ and therefore for sufficiently small $k(=2\pi/\Lambda$, or sufficiently large capillary wavelengths Λ) $\omega^2<0$ and the wetting layer is unstable to these modes. Specifically the nonequilibrium wetting layer is unstable to capillary wave fluctuations on the $\alpha\beta$ interface with wavelengths greater than the critical wavelength [20]

$$\Lambda_c=\left[\frac{-2\pi^2\sigma_{\alpha\beta}}{\partial F/\partial d}\right]^{1/2}, \tag{9}$$

where the characteristic lifetime of the nonequilibrium state is approximately given by [20]

$$\tau_L=\frac{24\sigma_{\alpha\beta}\eta}{d^3\left[\frac{\partial F}{\partial d}\right]^2}, \tag{10}$$

where η is the shear viscosity. The film rupture time τ_r is related to the lifetime by $\tau_r\sim f\tau_L$ with $f\sim7$. Therefore for $t\sim1.0\times10^{-3}$, $d\sim43.1$ nm, $\partial F/\partial d\sim-1.5\times10^5$ dyn/cm^3 (estimated from Fig. 2) and the values of $\sigma_{\alpha\beta}$ and η given in Table II we obtain $\tau_r\sim1.3\times10^4$ s which agrees qualitatively with the observed rupture time of $\tau_r=\tau_2-\tau_1\sim2.3\times10^4$ s from Fig. 5.

V. DISCUSSION

In this paper we examined the time-development of wetting droplets at the liquid-vapor surface of a critical hexadecane plus acetone mixture after they have coalesced into a uniform nonequilibrium wetting film, or perhaps more realistically, into a large nonequilibrium wetting droplet with size greater than the laser beam probe size. The nonequilibrium wetting film has a typical thickness of 43.1 ± 2.7 nm; this film ruptures after $\sim2.3\times10^4$ s to a thinner film of thickness 29.5 ± 2.0 nm. We explained the rupture of the nonequilibrium wetting film in terms of a hydrodynamic instability. The nonequilibrium film thickness is in a region where the disper-

sion force per unit area $F(d)$ is positive and $\partial F(d)/\partial d$ is negative (Fig. 2) and therefore this film is unstable to long wavelength capillary wave fluctuations on the adjacent critical $\alpha\beta$ interface. We believe that the thinner film corresponds to an equilibrium film. It gives reasonable agreement with the theoretical thickness of ~ 26 nm. We attribute the difference between the experimental and theoretical equilibrium film thickness to either our neglect of critical adsorption effects or to our uncertainty in the dielectric dispersion $\varepsilon(\omega)$.

We do not believe that the slight discrepancy, for the equilibrium film thickness between theory and experiment, is caused by a high impurity ion concentration which would screen the static contribution ($j=0$) to $F(d)$. For example, if one uses (5) to obtain better agreement between theory and experiment a value of $k_D^{-1}=40$ nm would be required for the Debye screening length. This value corresponds to an impurity ion concentration of 9×10^{21} m^{-3} assuming monovalent impurity ions of identical equivalent conductance in the two bulk liquid phases. However with this value of k_D one finds that $\partial F(d)/\partial d$ is positive for all d, namely, the wetting layer is stable to all capillary wave fluctuations on the adjacent $\alpha\beta$ interface. Hence in the presence of this impurity ion concentration there would be no explanation for the observed hydrodynamic instability. Further experimental work is required to see if impurity ions remove the instability as suggested by this analysis.

Finally we note that the thickness of the nonequilibrium wetting film is determined by quite different physics compared with the equilibrium film, where the latter is determined by Eq. (1). This can be understood as follows. The excess free energy $\mathcal{F}$ to form a β wetting droplet at an αv liquid-vapor surface [Fig. 1(b)] is given by [21]

$$\mathcal{F}\approx -S\pi r^2+\mathcal{L}2\pi r+\frac{W\pi r^2}{d^2}+\Delta\rho gLV\ , \tag{11}$$

where the droplet has lateral radius r, thickness d, and volume $V=\pi r^2 d/2$. Here we have assumed a spherical cap-shaped droplet of *small* contact angle where the spreading pressure $S=\sigma_{\alpha v}-\sigma_{\beta v}-\sigma_{\alpha\beta}$, σ_{ij} is the surface tension between phases i and j, $\mathcal{L}$ is the droplet line tension, W/d^2 is the nonretarded dispersion contribution with W the Hamaker constant, and the last term is the gravitational energy. The droplet shape kinetics will be faster than the diffusion-limited droplet growth kinetics; therefore a droplet will change shape at constant volume in order to minimize the free energy. Minimizing $\mathcal{F}$ at constant V gives the two-dimensional Laplace equation [21]

$$\mathcal{L}\sqrt{\pi h/2V}-S+\frac{3W}{d^2}=0 \tag{12}$$

which in the limit of large wetting layer droplets (large V) reduces to

$$d=\sqrt{3W/S}\ . \tag{13}$$

Namely the thickness of the droplet is determined by a competition between the spreading pressure and the dispersion force. This can be contrasted with the equilibrium film thickness (1) which is determined by a competition between the gravitational force and the dispersion force. For the conditions of Fig. 5 where $t=1.3\times 10^{-3}$, we use an effective Hamaker constant $W=W_0 t^{\beta}$ where $W_0\sim 2.9\times 10^{-16}$ erg [20], and $S\approx S_0 t^{\beta_1}$, where $S_0\sim 0.007$ erg/cm^2 [21] while β (≈ 0.33) and β_1 (≈ 0.83) are critical exponents. From (13) we determine that $d\sim 20$ nm for the nonequilibrium wetting layer thickness which is in qualitative agreement with the observed value of ~ 43.1 nm. Note that we should not expect quantitative agreement between this simple theory and experiment because (13) is only valid in the limit of small contact angles and nonretarded disperison forces. As has been discussed in a previous publication [20] when $d\sim 40$ nm for hexadecane plus acetone the dispersion force cannot be described simply in terms of a nonretarded form because the static and optical contributions to the dispersion force have opposite signs and differing d dependences. Therefore we are only able to use an effective Hamaker constant in this thickness range. We will consider these limitations in a future publication.

ACKNOWLEDGMENT

This work was supported in part by the National Science Foundation through Grant Nos. DMR-9208123 and DMR-9223872.

[1] J. W. Cahn, J. Chem. Phys. **66**, 3667 (1977).
[2] C. Ebner and W. F. Saam, Phys. Rev. Lett. **38**, 1486 (1977).
[3] For reviews, see S. Dietrich, in *Phase Transitions and Critical Phenomena,* edited by C. Domb and J. Lebowitz (Academic, London, 1987), Vol. 12; D. E. Sullivan and M. M. Telo da Gama, in *Fluid Interfacial Phenomena,* edited by C. A. Croxton (Wiley, New York, 1985); M. Schick, in *Liquids at Interfaces,* Les Houches, Session XLVIII, 1988, edited by J. Charvolin, J. F. Joanny, and J. Zinn-Justin (North-Holland, Amsterdam, 1990).
[4] See, for example, R. F. Kayser, M. R. Moldover, and J. W. Schmidt, J. Chem. Soc. Faraday Trans. 2 **82**, 1701 (1986) and references therein.
[5] I. E. Dzyaloshinskii, E. M. Lifshitz, and L. P. Pitaevskii, Adv. Phys. **10**, 165 (1961).
[6] B. M. Law, Phys. Rev. Lett. **69**, 1781 (1992).
[7] Note that we are not considering *ionizable surfaces* which was the subject of two papers by Kayser: R. F. Kayser, Phys. Rev. Lett. **56**, 1831 (1986); J. Phys. (Paris) **49**, 1027 (1988).
[8] J. Mahanty and B. W. Ninham, *Dispersion Forces* (Academic, London, 1976), Chap. 7. We have converted from an energy per unit area E given by Mahanty and Ninham to a force per unit area F [Eq. (5)], using $F=\partial E/\partial d$.
[9] P.-G. de Gennes, J. Phys. (Paris) Lett. **42**, L377 (1981).
[10] R. F. Kayser, Phys. Rev. B **34**, 3254 (1986).

[11] D. Ripple and C. Franck, Phys. Rev. B **40**, 7279 (1989).
[12] J. N. Israelachvili, *Intermolecular and Surface Forces* (Academic, London, 1985), p. 144.
[13] D. Beaglehole, in *Fluid Interfacial Phenomena,* edited by C. A. Croxton (Wiley, New York, 1985).
[14] S. Fisk and B. Widom, J. Chem. Phys. **50**, 3219 (1969).
[15] M. Born and E. Wolf, *Principles of Optics* (Pergamon, Oxford, 1980), Sec. 1.6; B. M. Law and D. Beaglehole, J. Phys. D **14**, 115 (1981); B. M. Law, Ph.D. thesis, Victoria University of Wellington, New Zealand, 1985.
[16] D. S. P. Smith and B. M. Law (unpublished).
[17] M. E. Fisher and P.-G. de Gennes, C. R. Acad. Sci. Ser. B **287**, 207 (1978).
[18] A. J. Liu and M. E. Fisher, Phys. Rev. A **40**, 7202 (1989).
[19] A. Vrij, Discuss. Faraday Soc. **42**, 23 (1966); A. Vrij and J. Th. G. Overbeek, J. Am. Chem. Soc. **90**, 3074 (1968).
[20] B. M. Law, Phys. Rev. E **48**, 2760 (1993).
[21] B. M. Law. Phys. Rev. Lett. **72**, 1698 (1994).
[22] F. Buckley and A. A. Maryott, *Tables of Dielectric Dispersion Data for Pure Liquids and Dilute Solutions,* Natl. Bur. Stand. (U.S.) Circ. No. 589 (U.S. GPO, Washington, D.C., 1958).
[23] *International Critical Tables,* edited by E. W. Washburn, C. J. West, N. E. Dorsey, and M. D. Ring (McGraw-Hill, New York, 1930), Vol. VII, p. 35.
[24] D. B. Hough and L. R. White, Adv. Colloid Interface Sci. **14**, 3 (1980).
[25] I. L. Pegg, Ph.D. thesis, University of Sheffield, 1982.
[26] *CRC Handbook of Chemistry and Physics,* 66th ed., edited by R. C. Weast, M. J. Astle, and W. H. Beyer (Chemical Rubber, Boca Raton, 1985).
[27] E. Brezin, J. C. Le Guillou, and J. Zinn-Justin, Phys. Lett. **47A**, 285 (1974); H. B. Tarko and M. E. Fisher, Phys. Rev. Lett. **31**, 926 (1973); A. J. Liu and M. E. Fisher, Physica A **156**, 35 (1989).
[28] M. R. Moldover, Phys. Rev. A **31**, 1022 (1985); H. L. Gielen, O. B. Verbeke, and J. Thoen, J. Chem. Phys. **81**, 6154 (1985).